The Archibald Ultracentrifugation Method in the Study of Macromolecules (Special Issue on Polymer Chemistry, I)

AUTHOR(S):

Kotaka, Tadao; Inagaki, Hiroshi

The Archibald Ultracentrifugation Method in the Study of Macromolecules

Tadao KOTAKA and Hiroshi INAGAKI*

(Inagaki Laboratory)

Received March 5, 1964

CONTENTS

I. INTRODUCTION

Ultracentrifugation, which was first brought into use by Svedberg and his associates (1923a, b; 1940) some forty years ago, is now one of the most important physical method in the study of macromolecules. In the last fifteen years great advances have been made in instrumentation, experimental technique (cf. Schachman, 1959) and also in the fundamental theory necessary for the analysis of data (cf. Williams et al., 1958; Baldwin and Van Holde, 1960; Fujita, 1962). These advances have made it possible to obtain a vast amount of valuable information about macromolecular systems such as: molecular weights and thermodynamic properties (sedimentation equilibrium method), sedimentation coefficients and molecular weight distributions (sedimentation velocity method), equilibrium and rate constants of macromolecular reactions (sedimentation in chemically reacting system), bouyant densities and heterogeneity [density gradient sedimentation method (cf. Vinograd and

* 小高 忠男, 稲垣 博

Hearst, 1962)].

One of these is the Archibald method for the determination of molecular weights. This method, first introduced by Archibald (1947b), is based on use of the boundary condition for the ultracentrifuge in the transient period during approach to sedimentation equilibrium. Chief advantages of this method are not only that it requires only small amounts of materials, as all the other ultracentrifugation methods do, but also that it is rapid and fairly accurate.

The original theory of Archibald dealt with ideal, monodisperse or polydisperse systems. This has been successfully applied to measuring molecular weights, particularly of proteins. Trautman (1956) introduced a procedure sensitive to detecting the heterogeneity and nonideality of the system. Subsequently Kegels, Klainer and Salem (1957) extended the Archibald method to nonideal, polydisperse systems and indicated that a parameter for measuring nonideality of the solution at low concentrations can be obtained as well as the weight-average molecular weight of the polydisperse solute. Kegels and Rao (1958) showed that this method is also applicable to chemically reacting systems and determined equilibrium constants of association and dissociation reaction of macromolecules (Rao and Kegels, 1958). A detailed discussion on the effect of heterogeneity in ideal polydisperse systems was made by Yphantis (1959), who indicated the types of average molecular weights to be obtained by this method. More recently Fujita et al. (1962) also made an extension of the Archibald method to nonideal, polydisperse solutions on the basis of the thermodynamics of irreversible processes (Hooyman, 1956b). Fujita et al. (1962) have indicated that the new theory allows determination of the weight-average molecular weight and the light scattering second virial coefficient of the given system. Experimental studies by them on dilute solutions of synthetic macromolecules have yielded important evidence for the validity of the generalized theory. One may now use this method as a routine procedure for determining the weight-average molecular weight and the second virial coefficient of nonideal, polydisperse systems.

The scope of the present review embraces the current situation of the Archibald method in both theoretical and experimental aspects. This discussion will be given on the basis of the generalized theory. Some remarks will also be made on the practice of the Archibald method. However we do not intend to mention about the details of experimentation such as the description of the ultracentrifuges and experimental techniques. Rather we will confine ourselves to the discussion on how to analyze the data to obtain the pertinent information on the subject. Some of the important experimental results so far obtained will also be cited.

II. THEORY

1. The Archibald Theory

The Archibald method is based on use of the boundary condition of the

centrifuge cell. The correct boundary condition has been known from the earliest days of research (Mason and Weaver, 1924; Faxén, 1929). However until Archibald (1947a, b) pointed it out with numerical illustrations the full significance of its being used for measuring molecular weights was not realized. The situation can be most easily visualized by considering the kinematic picture of the centrifugation of a solution.

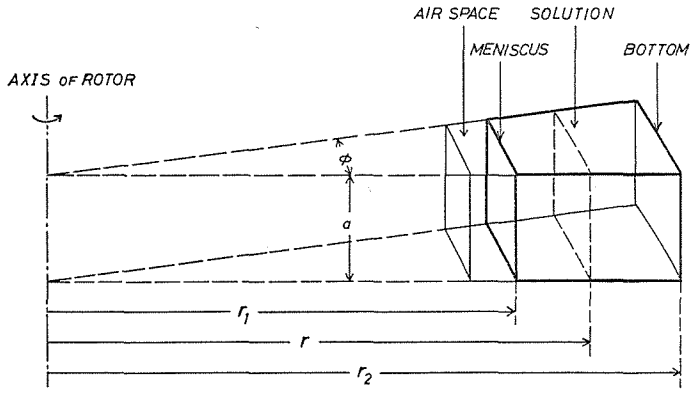

Fig. 1. Schematic diagram of a sector-shaped ultracentrifugal cell. The angle, ϕ, is usually 4°, but smaller angles are often used. The distance a represents the optical path in the cell, i. e., the thickness of the solution column. The area of the cylindrical surface at the distance r is $A=ar\phi$.

We first consider a two component system which is subjected to centrifugation in a sector-shaped cell rotated at a constant speed and at a constant temperature. Fig. 1 schematically shows the cell in which the solution is bounded between the distance r_1 (the meniscus) and r_2 (the bottom) from the axis of rotation. Now let us suppose a cylindrical surface of area A at the distance r. The amount of solute transported per unit time across the surface by sedimentation, dm_s/dt, is given by

$$dm_s/dt = Acs\omega^2 r \tag{1}$$

where

c = the local concentration of the solute in g/ml;
s = the sedimentation coefficient of the solute in sec;
ω = the angular velocity of the rotor in radian/sec.

There is also transport of the solute in the opposite direction due to diffusion, the amount of which, dm_D/dt, can be written by use of Fick's first law of diffusion (1855) as

$$dm_D/dt = -AD(\partial c/\partial r). \tag{2}$$

where

D = the diffusion coefficient of the solute in cm^2/sec.

The sum of these two terms gives the net amount of solute transported across the surface in the centrifugal direction. By dividing this by the area A we obtain the flow equation

$$J = cs\omega^2 r - D(\partial c/\partial r) \tag{3}$$

where

J = the flow of solute relative to the cell: the amount, in gram per ml, transported across unit area at the distance r in unit time.

In the similar manner one can calculate the flow across the surface at the distance $r+dr$. Subtraction of the second from the first [eq. (3)] gives the net accumulation of solute per unit time in the volume element bounded by two cylindrical surfaces at the distance r and $r+dr$, respectively. This leads to the well-known Lamm equation of sedimentation (cf. Schachman, 1959, p. 11)

$$\frac{\partial c}{\partial t} = -\frac{1}{r}\frac{\partial}{\partial r}(rJ) = \frac{1}{r}\frac{\partial}{\partial r}\left[r\left(D\frac{\partial c}{\partial r} - cs\omega^2 r\right)\right] \tag{4}$$

The boundary condition is as follows: since there is no transport of materials into or out of the cell, there should be no flow of any component across either end of the solution column, that is

$$J = 0 \text{ at } r = r_1 \text{ and } r_2 \text{ for anytime } t. \tag{5}$$

The application of this condition to the flow equation (3) leads to

$$\omega^2 s/D = [(1/rc)(\partial c/\partial r)]_{r=r_1 \text{ and } r_2}. \tag{6}$$

This boundary condition does not imply that there is *no change* of concentration with time at the ends. There is actually depletion and accumulation of the solute at the meniscus and the bottom, respectively, and c and $(\partial c/\partial r)$ vary continuously with time. The change, however, should occur in such a manner that $(1/rc)(\partial c/\partial r)$ remains constant at both ends of the column. In fact Archibald (1947) demonstrated with his solution to the Lamm equation that this is the case.

The equation (6) shows that if one can measure $(1/rc)(\partial c/\partial r)$ at the ends, then the ratio (s/D) and subsequently the molecular weight of the solute can be obtained by use of the Svedberg equation [cf. Svedberg and Pedersen, 1940].

Equation (6) applies practically only for monodisperse, ideal solutions. Archibald (1947) pointed out that in case of a polydisperse, (ideal) solution the obtained (s/D) is the weight-average value, so that the molecular weight is the weight-average provided $\bar{v}$ is equal for all solutes.

Solutions of synthetic macromolecules are usually polydisperse, nonideal systems. More rigorous expressions should be required to describe such flows; these will be discussed in the subsequent section.

2. Extension of the Archibald Theory to Polydisperse, Nonideal Systems

We now consider a rotating system in a centrifuge at constant temperature with a nonideal, incompressible solution which consists of a single solvent (designated as component 0) and q species of solutes (designated as components 1, 2,……, q). We introduce the symbols

ρ = local density of the solution;

c_i=local concentration of solute $i(i=1, 2, \cdots\cdots, q)$ in gram per ml of solution;

$\bar{v}_i$=partial specific volume of solute i;

μ_i=chemical potential of solute i per gram;

J_i=flow of solute i relative to the cell: the amount, in gram per ml, transported across unit area at the distance r in unit time.

From the theory of the thermodynamics of irreversible processes (Hooyman et al., 1953; Hooyman, 1956a, b) the flow, J_i, can be represented by

$$J_i=\sum_{k=1}^{q} L_{ik}[(1-\bar{v}_k\rho)\omega^2 r-\sum_{j=1}^{q}\mu_{kj}(\partial c_j/\partial r)] \qquad (7)$$
$$(i=1, 2, \cdots\cdots, q)$$

with

$$\mu_{kj}=(\partial\mu_k/\partial c_j)_{T, P, c_{m(m\neq 0, j)}} \qquad (7a)$$

where T is the absolute temperature, P is the pressure at the position and the time being considered. The coefficients L_{ik} are called phenomenological coefficients and are analogous to the practical sedimentation and diffusion coefficients which are obtained experimentally (Hooyman, 1956b). We further assume all solutes to be non-electrolyte and expand the excess chemical potential in power series in the concentration c_i

$$\mu_k=\mu_k^0+(RT/M_k)\ln(c_k y_k) \qquad (7b)$$

$$\ln y_k=M_k\sum_{i=1}^{q} B_{ki}c_i+\text{higher terms in } c_i, \qquad (7c)$$
$$(k=1, 2, \cdots\cdots, q)$$

with

y_k=the activity coefficient, in g/ml scale, of solute k.

Here again the boundary condition, $J_i=0$ for *any* solute i at $r=r_1$ and r_2, applies to equation (7), which yields a set of q-equations (Kegels et al., 1957; Fujita et al., 1962)

$$\frac{\partial c_i}{\partial r}=\frac{c_i M_i(1-\bar{v}_i\rho)\omega^2 r}{RT}-c_i\sum_{k=1}^{q}\frac{\partial \ln y_i}{\partial c_k}\left(\frac{\partial c_k}{\partial r}\right). \qquad (8)$$
$$(i=1, 2, \cdots\cdots q;\ r=r_1 \text{ and } r_2).$$

These equations are similar in their appearance with the basic equations for sedimentation equilibrium (cf. Baldwin et al., 1960, p 467) of a polydisperse, nonideal solution. However a distinction should be made between them. The Archibald equation (8) is only valid at either end of the column, $r=r_1$ and r_2, for any time t. While the equilibrium equation is derived from the condition $J_i=0$ [more accurately $\partial c_i/\partial t=0$] $(i=1, 2, \cdots\cdots, q)$ anywhere in the cell and valid for any value of r and independent of time t. This implies that the latter provides a set of differential equations to determine c_i as a function of r, while the former provides a set of algebraic relations for the values of c_i and $(\partial c_i/\partial r)$ at either $r=r_1$ or r_2.

By solving equation (8) with resqect to $(\partial c_i/\partial r)$ we obtain

$$(RT/\omega^2 r)(\partial c_i/\partial r) = (1-\bar{v}_i\rho)c_i M_i - \sum_{j=1}^{q}(1-\bar{v}_j\rho)M_i M_j B_{ij} c_i c_j + (\text{higher terms in } c_i) \quad (i=1, 2, \cdots\cdots, q;\ r=r_1 \text{ and } r_2). \tag{8a}$$

In the ultracentrifuge in common use, the concentration distribution is measured in terms of the refractive index increment. We therefore introduce a variable

$$\tilde{n} = \sum_{i=1}^{q} R_i c_i \tag{9}$$

with

R_i = the specific refractive index increment of solute i.

We obtain an equation for the measurable quantity $(\partial\tilde{n}/\partial r)$ by multiplying equation (8a) by R_i and summing up for all solute components. Further dividing this by $\tilde{n}$ we finally obtain the equation

$$\frac{RT}{\omega^2 r}\frac{1}{\tilde{n}}\frac{\partial\tilde{n}}{\partial r} = \sum_{i=1}^{q} R_i M_i^* c_i / \sum_{i=1}^{q} R_i c_i - c\sum_{i=1}^{q}\sum_{j-1}^{q} M_i M_j^* B_{ij} R_i c_i c_j / \sum_{i=1}^{q}\sum_{j=1}^{q} R_i c_i c_j + (\text{highter terms in } c_i) \quad (r=r_1 \text{ and } r_2) \tag{10}$$

with

$$c = \sum_{i=1}^{q} c_i, \tag{10a}$$

$$M_i^* = (1-\bar{v}_i\rho)M_i. \tag{10b}$$

Further simplification of equation (10) is possible if one assumes that all solutes components have the same partial specific volume $\bar{v}(=\bar{v}_i$ for all solutes $i)$ and the same specific refractive index increment $\bar{R}(=R_i$ for all solutes $i)$. This assumption is quite justifiable for homologous macromolecules. By introducing this assumption into equation (10) we obtain

$$M_{app}(t) = \sum_{i=1}^{q} M_i c_i/c - c\sum_{i=1}^{q}\sum_{j=1}^{q} M_i M_j B_{ij} c_i c_j / c^2 + \text{higher terms in } c \quad (r=r_1 \text{ and } r_2). \tag{11}$$

The quantity $M_{app}(t)$ has the dimension of molecular weight and is defined by measurable quantities as

$$M_{app}(t) = RT(\partial\tilde{n}/\partial r)/\omega^2 r(1-\bar{v}\rho)\tilde{n} \quad (r=r_1 \text{ and } r_2). \tag{11a}$$

It should be noted that equation (11) is referred to the state at the given position, specifically at the meniscus or the bottom at the given time t. The local concentration varies with time until finally the equilibrium state is attained. Since sedimentation concentrates heavier solutes at the bottom, the local distribution of the solutes is also a function of time. Therefore $M_{app}(t)$ needs to be extrapolated back to zero time to obtain a quantity referring to the initial state of the solution. Thus we obtain

$$M_{app} \equiv M_{app}(0) = M_w[1 - M_w B c^0 + \text{higher terms in } c^3]. \tag{12}$$

Here c^0 is the value of c for the initial solution (i.e., the total concentration of the solution before centrifugation), M_w is the weight-average molecular weight defined by

$$M_w=\sum_{i=1}^{q} M_i f_i \tag{12a}$$

and B is a nonideality parameter defined by

$$B=\sum_{i=1}^{q}\sum_{j=1}^{q} M_i M_j B_{ij} f_i f_j/(M_w)^2. \tag{12b}$$

In the above equations, f_i denotes the weight fraction of solute i in the initial solution. The quantity M_{app} is termed the apparent molecular weight of the solute. The values of M_{app} for both ends of the cell should agree with each other; this is because all terms in right-hand side of equation (12) are independent of r (provided the pressure effect is negligible).

Equation (12) may alternatively be written in the form

$$1/M_{app}=1/M_w+Bc^0+\text{higher terms in } c^0. \tag{13}$$

The procedure required here is first to evaluate $\tilde{n}$ and $(\partial\tilde{n}/\partial r)$ at either ends of the cell obtained at various times of centrifugation with a constant velocity of rotation; to calculate $M_{app}(t)$ by equation (11a) with relevant data; then to extrapolate $M_{app}(t)$ to zero time to obtain M_{app}; and finally to plot $1/M_{app}$ against the initial concentration, c^0. The plot for $1/M_{app}$ versus c^0 should allow evaluation of M_w from its intercept at $c^0=0$, and of B from its initial slope.

3. Comparison with Light Scattering Virial Expansion

From the fluctuation theory of the turbidity of polydisperse systems (Kirkwood and Glodberg, 1950; Stockmayer, 1950) the turbidity due to the composition fluctuation, τ_c, can be written by using the same definitions as in the previous section

$$\tau_c=\frac{32\pi^3 n^2}{3\lambda_0^4 N_A}\left[\sum_{i=1}^{q} R_i^2 c_i M_i-\sum_{i=1}^{q}\sum_{j=1}^{q} M_i M_j B_i B_j R_i R_j c_i c_j+\text{higher terms in } c_i\right]. \tag{14}$$

Here the additional symbols introduced are

n = the refractive index of the solution;

λ_0 = the wave length of the light (in vaccum) from the light source;

N_A = the Avogadro number.

Again we assume $R_i=\overline{R}$ for all solutes. We note that the usually measured quantity in the light scattering method, the reduced intensity of scattered light at zero angle of incidence, i_0, is approximately related to the turbidity, τ_c as $\tau_c=(16\pi/3)i_0$. Then i_0 can be written in the familiar virial form

$$\frac{Kc^0}{i_0}=\frac{1}{M_w}+2A'_2c^0+\text{higher terms in } c^0 \tag{15}$$

with

$$K=2\pi^2 n^2(\overline{R})^2/\lambda_0^4 N_A \tag{15a}$$

$$A'_2=\frac{1}{2}\sum_{i=1}^{q}\sum_{j=1}^{q}M_iM_jB_{ij}f_if_j/(M_w)^2 \qquad (15b)$$

where K is the well-known light scattering factor and A'_2 is the so-called light scattering virial coefficient. It is quite obvious that from comparison of equations (15) and (15b) to equations (13) and (12b), respectively, the Archibald method of plotting $1/M_{app}$ versus c^0 is equivalent to the light scattering virial expansion: in the plot of $1/M_{app}$ versus c^0; the intercept and the initial slope give weight-average molecular weight and twice the second virial coefficient of light scattering, respectively (Fujita et al., 1962).

III. PRACTICAL PROCEDURE

1. Introductory Remarks

Ultracentrifuges now in common use furnish either one or both schlieren and Rayleigh interference optics to measure the distribution of solutes in the cell (cf. Schachman, 1959). The schlieren optical system provides a gradient curve, an example is shown in Fig. 2, in which height from the base-line is proportional to $(\partial\tilde{n}/\partial r)$ at the position r as defined by

$$(\partial\tilde{n}/\partial r)=\frac{(\tan\theta)\Delta y}{abG_y}, \qquad (16a)$$

$$r=x/G_x. \qquad (16b)$$

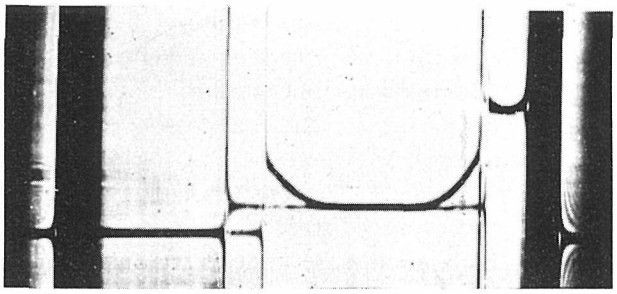

Fig. 2. An example of a gradient curve obtained with a schlieren optical system. A sucrose-water system (c^0=4.480 g/dl) was centrifuged at 25° with 42,040 rpm in a Spinoco-E ultracentrifuge. A double sector cell was employed. A slightly lesser amount of Fluorochemical FC 43 (as a bottom liquid) and larger amount of solvent were placed into the reference side of the cell than in the solution side so that two menisci and bottom lines can be seen. [By the courtesy of Dr. F. E. LaBar (1963)].

The definition of the symbols are

G_x=total radial magnification
=magnification of schlieren camera lens times the magnification of the projector;
G_y=magnification of the schlieren lens times the magnification of the projector;
a=optical path of the cell;
b=optical lever arm;

x=magnified radial dstance;

Δy=height of the solution pattern from the base-line at the distance x;

θ=the angle the schieren diaphragm makes with the light source.

The Rayleigh interference optical system, on the other hand, provides a Rayleigh fringe picture, an example is shown in Fig. 3, in which the number of fringes, j, crossed in the radial direction between any two position gives the difference in refractive index, $\Delta\tilde{n}$, by

$$\Delta\tilde{n}=j\lambda/a \tag{17}$$

where λ is the wavelength of the monochromatic light from the light source.

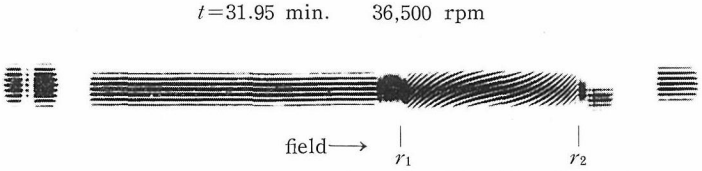

Fig. 3. An example of a fringe pattern obtained with a Rayleigh interference optical system. A sucrose-water system (c^0=5.424 g/dl) was centrifuged at 25° with 35,600 rpm. in a Spinco-E ultracentrifuge. A small amount of 1-3-butanediol was added to the water in the reference side of the cell to raise the refractic index of the reference, because a very blurred fringe pattern would result in an experiment if the difference in refractive index were too large between the solution and the reference side of the cell. [By the courtesy of Dr. F. E. LaBar (1936)].

As the theory mentions, one has to evaluate the values of $(1/r\tilde{n})(\partial\tilde{n}/\partial r)$ at the meniscus and the bottom from schlieren and/or Rayleigh patterns obtained at various times during a sedimentation experiment. Various procedures have been proposed so far for this purpose. Each method has its *pro* and *cons*; and unfortunately, we feel we can not point out any particular method as the best reliable one. Therefore we will try rather to give some unbiased comments on these procedures.

One more thing which should be added here is that although it is preferable to use data from both ends and to test the coincidence of M_{app} obtained from both ends, one is often obliged to use data only from the meniscus. This is mainly due to the fact that the accumulation of solutes gives rise to very steep concentration gradients at the bottom and this obscures the correct location of the bottom. To avoid this difficulty a small amount (perhaps 0.1 ml) of a dense, solvent-immiscible, transparent liquid is first introduced into the cell, and thereafter the solution to be tested is added (Ginsburg et al., 1956). This procedure provides a fairly sharp interface between the solution and the bottom liquid. As such bottom liquids, Dow-Corning No. 555 Silicone oil (Ginsburg et al., 1956), Kel-F Polymer oil (Van Holde and Baldwin, 1958) and Fluorochemical FC-43 (Yphantis, 1959) are commonly employed for aqueous solutions. For organic solvents it seems that no satisfactory bottom liquids yet exist. In a few cases dehydrated glycerine was employed for organic solvents such as methyl ethyl ketone (Fujita et al., 1962), cyclohexane and *n*-buthylchloride (Inagaki et al., 1963a).

2. Determination of $M_{app}(t)$

a) Use of schlieren optics. From a photograph of gradient curve vaules of $(\partial\tilde{n}/\partial r)$ are measured directly. The value of $\tilde{n}$ at $r=r_1$ and r_2 can be calculated by the procedure developed by Klainer and Kegels (1955). During early stages of centrifugation in which a plateau region still exists in the cell (cf. Fig. 4) the value of $\tilde{n}$ at $r=r_1$ and r_2 are

$$(\tilde{n})_{r_1}=\tilde{n}^0-\left(\frac{1}{r_1^2}\right)\int_{r_1}^{r_p} r^2\left(\frac{\partial\tilde{n}}{\partial r}\right)dr \tag{18a}$$

$$(\tilde{n})_{r_2}=\tilde{n}^0+\left(\frac{1}{r_2^2}\right)\int_{r_p}^{r_2} r^2\left(\frac{\partial\tilde{n}}{\partial r}\right)dr \tag{18b}$$

where

$\tilde{n}^0$=the refractive index increment of the initial solution;

r_p=radial distance of any arbitrary point in the plateau region.

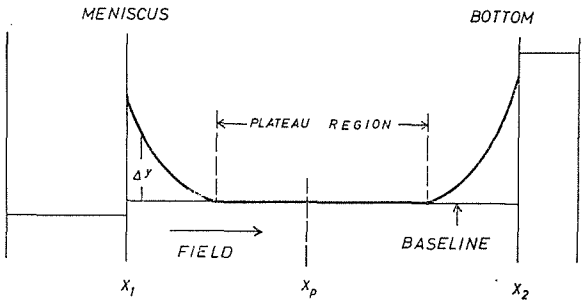

Fig. 4. Schematic diagram of a typical schlieren picture in which the plateau region still exists (cf. Fig. 2). Only the solution side is indicated.

In later stages in which the plateau region has vanished evaluation of $\tilde{n}$ at $r=r_1$ and r_2 involves more the laborious calculations

$$(\tilde{n})_{r1}=\tilde{n}^0+\frac{1}{(r_2^2-r_1^2)}\int_{r_1}^{r_2}(r^2-r_2^2)(\partial\tilde{n}/\partial r)dr \tag{19a}$$

$$(\tilde{n})_{r2}=\tilde{n}^0+\frac{1}{(r_2^2-r_1^2)}\int_{r_1}^{r_2}(r^2-r_1^2)(\partial\tilde{n}/\partial r)dr. \tag{19b}$$

The value of $\tilde{n}^0$ in equations (18a)-(19b) can be evaluated by employing a synthetic boundary cell to layer the solvent onto the solution of known initial concentration c^0 (cf. Schachman, 1959), and by carrying out the calculation

$$\tilde{n}^0=\int_{r_1}^{r_p}(\partial\tilde{n}/\partial r)dr. \tag{20a}$$

(Perhaps it is better to take a series of pictures successively and extrapolate $\tilde{n}^0$ back to zero time). Here r_p is the distance of any arbitrary position in the plateau region ahead of the boundary.

This can also be evaluated by doing a separate sedimentation velocity experiment at high enough velocity to form a complete boundary separated from the meniscus and calculating the area under the boundary by

$$\tilde{n}^0=\int_{r_1}^{r_p}\left(\frac{r}{r_1}\right)^2(\partial\tilde{n}/\partial r)\,dr. \tag{20b}$$

It should be noted that in equation (20a) the correction for radial dilution effect is not involved, since the concentration change across the boundary made by layering a solvent onto a solution of the initial concentration c^0 is exactly equal to c^0 at time $t=0$. Whereas in case of the boundary formed by a sedimentation velocity run, the correction factor $(r/r_1)^2$ is required as in equation (20b).

b) **Use of Rayleigh interference optics.** In the case where there still exists a plateau region (where the fringes are all parallel to the radial direction), counting the fringes from plateau to either the meniscus or the bottom gives $(\tilde{n})_{rp}-(\tilde{n})_{r1}$ or $(\tilde{n})_{r2}-(\tilde{n})_{rp}$, respectively. The change of concentration in terms of $\tilde{n}$ at the plateau region is followed readily by observing the lateral movement of the fringes with time across the pattern. This gives the relation between $(\tilde{n})_{rp}$ and $\tilde{n}^0$ (Richards and Schachman, 1959).

The values of $(\tilde{n})_{r1}$ and $(\tilde{n})_{r2}$ can also be obtained, if one does not mind doing a little calculation, by

$$(\tilde{n})_{r1}=\tilde{n}^0-[r_2^2(\Delta\tilde{n})_t-\int_{r_1}^{r_2}r^2d(\Delta\tilde{n})]/(r_2^2-r_1^2) \tag{21a}$$

$$(\tilde{n})_{r2}=\tilde{n}^0-[r_1^2(\Delta\tilde{n})_t-\int_{r_1}^{r_2}r^2d(\Delta\tilde{n})]/(r_2^2-r_1^2)=(\tilde{n})_{r1}+(\Delta\tilde{n})_t \tag{21b}$$

where

$(\Delta\tilde{n})_t$ = difference in $\tilde{n}$, which is directly proportional to the total number of fringes, between the meniscus and the bottom.

The number of fringes corresponding to $\tilde{n}^0$ is determined as in the schlieren method by a layering technique with a synthetic boundary cell, which requires merely counting the number of fringes from the meniscus to the bottom along the radial direction.

With these optics, counting the number of fringes is the only procedure required for evaluating $\tilde{n}$. However for evaluating $(\partial\tilde{n}/\partial r)$ at r_1 and r_2 it is necessary to perform numerical differentation of fringe number with respect to r.

c) **Further remarks.** One often claims that the evaluation of $(\partial\tilde{n}/\partial r)$ at the ends is straightforward especially with the use of the schlieren method. In practice, however, it is not quite that easy. Direct reading of $(\partial\tilde{n}/\partial r)$ from a schlieren picture can be safely done only as close as 0.03 cm apart from the ends. With the Rayleigh method the numerical differentiation is involved here. In any case steep gradient usually found at the ends (this is particularly true at the bottom) introduces cretain ambiguity in evaluation of $(\partial\tilde{n}/\partial r)$. Since this quantity directly appears in the calculation of $M_{app}(t)$ [cf. equation (11a)], the ambiguity could be a serious source of error.

One possible method of avoiding this difficulty is to operate the centrifuge at rather low speeds so as not to form a very steep gradient at the ends. Another possibility is to run the centrifuge at high speed and wait for a while so that a complete boundary is almost formed and the $(\partial\tilde{n}/\partial r)$

curve becomes nearly horizontal at the meniscus with sacrifice of the data at the bottom (Ehrenberg, 1957). This method would be well applicable to monodisperse, ideal solutions. However, in any case where there is significant dependence of $M_{app}(t)$ on time (this is always true for nonideal solutions and sometimes for highly polydisperse solutions), one might not be able to extrapolate $M_{app}(t)$ back to zero time.

For providing the reliable estimation of $(1/r\tilde{n})(\partial\tilde{n}/\partial r)$ there are a few other methods now in use.

One method was introduced by Archibald (1947) himself: $(1/r\tilde{n})(\partial\tilde{n}/\partial r)$ at any r near the ends is plotted against r and evaluated at the ends by extrapolation. The value of $\tilde{n}$ at an arbitrary position r can be obtained from

$$(\tilde{n})_r=(\tilde{n})_{r_1}+\int_{r_1}^{r}(\partial\tilde{n}/\partial r)dr \qquad (22)$$

[for $(\tilde{n})_r$ near the bottom simply replace r_1 by r_2 in the above equation].

Archibald (1947b) gave a demonstration of this plot with his numerical data. Also Mommaerts and Aldrich (1958) applied this method to their experimental data obtained with Rayleigh optics. In both of these cases it was not quite certain that the plot of $(1/r\tilde{n})(\partial\tilde{n}/\partial r)$ versus r does give a straight line over a workable range near the ends. Never-the-less this procedure seems to provide reasonably good results (with uncertainly of about 5%) [Mommaerts and Aldrich, 1958; Richards and Schachman, 1959; for more discussion see Labar, 1963].

Fujita et al. (1962) found that in a polydisperse, nonideal solution, specifically a polystyrene-methyl ethyl ketone system, a plot of $\log[(1/r\tilde{n})(\partial\tilde{n}/\partial r)]$ versus r gave straight lines in a considerable range near the ends for the data obtained in early stage of centrifugation. An example of such plots is shown in Fig. 5. Scholtan and Marzolph (1962) found that in poly-

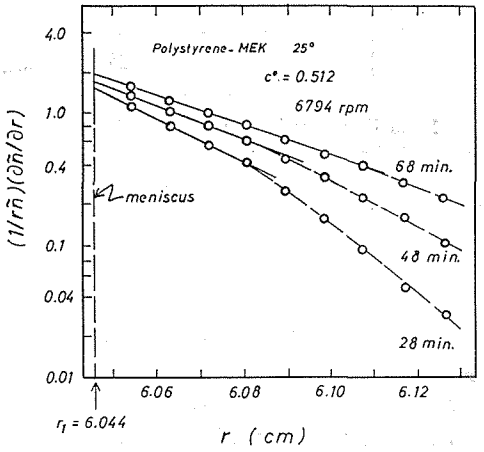

Fig. 5. Demonstration of the linearity in the plot of $\log[(1/r\tilde{n})(\partial\tilde{n}/\partial r)]$ versus r in the region near the meniscus. In this particular example polystyrene $H(M_w=4.76\times10^5)$-methyl ethyl ketone (0.512 g/dl) system was centrifuged at 25° with 6,794 rpm. The data were taken at various times as indicated. (Fujita et al., 1962).

acrylnitrile-dimethyl formamide system, a plot of $(\partial\tilde{n}/\partial r)$ versus r on a probability paper gave straight lines near the meniscus, particularly when bell-shaped gradient curves had appeared. At the moment these two are just empirical procedures, to which no theoretical justification has been given so far.

Another method consists of plotting $(\partial\tilde{n}/\partial r)$ versus r, evaluating $(\partial\tilde{n}/\partial r)$ at r_1 and r_2 first, and then calculating $(1/r\tilde{n})(\partial\tilde{n}/\partial r)$ at r_1 and r_2 (Ginsburg et al., 1956; Richards and Schachman, 1959; see also Peterson and Mazo, 1961; LaBar, 1963). Yphantis (1963: unpublished; cited in LaBar, 1963) worked out numerical solutions for sedimentation during the transient period (in a rectangular cell, constant field: Mason and Weaver, 1924) with an IBM computor. The results show that $(\partial\tilde{n}/\partial r)$ can be determined at the ends by linear extrapolation with high accuracy, provided the speed is appropriately low. A demonstration of this procedure was given by LaBar (1963) with a sucrose-water system (cf. Fig. 6), in which the molecular weight could be determined within 2% accuracy.

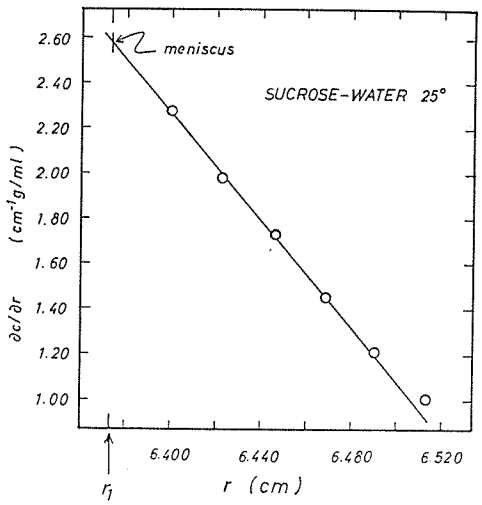

Fig. 6. Demonstration of the linearity in the plot of $\partial c/\partial r$ versus r in the region near the meniscus. A sucrose (M=342.3)-water (4.480 g/dl) system was centrifuged at 25° with 42,040 rpm. The data taken at 37.39 min. of centrifugation, while the plateau region was present. This particular data gave an observed value of M=348.3 (LaBar, 1963).

Because of the ease in evaluating $\tilde{n}$ with Rayleigh optics and $(\partial\tilde{n}/\partial r)$ with the schlieren optics, Richards and Schachman (1959) proposed to use both optics in single experiment.

Baldwin (1959) proposed a still another method for evaluating $M_{app}(t)$, which simply involves measurements of $\tilde{n}$ and r near the ends and use of the relation:

$$\lim_{r\to r_1}\frac{\ln[(\tilde{n})/(\tilde{n})_{r_1}]}{r-r_1}=\left(\frac{1}{\tilde{n}}\frac{\partial\tilde{n}}{\partial r}\right)_{r_1} \tag{23}$$

(for the bottom replace r_1 by r_2). Although not many tests have been carried out on this method, this seems to be a very interesting alternative particularly with use of the Rayleigh optics.

3. Extapolation of $M_{app}(t)$ to Zero Time

The next item required is the determination of M_{app} as a function of the initial concentration c^0. For doing this one has to extrapolate $M_{app}(t)$ [the quantity defined by equation (11a)] back to zero time. Here a question might arise on how to define the time of centrifugation. Any theory implicitly assumes a sudden jump of the rotor speed from zero to a desired value at $t=0$. In practice this is certainly not the case but rather there is a time required for acceleration of the rotor. Neither the time after the rotor is set into motion nor the time after the desired speed is attained is appropriate to be assigned as the time of centrifugation. One reasonable way of defining this is to introduce a zero time corection, Δt, as

$$\Delta t=\frac{1}{\omega^2}\int_0^{t_0}[\omega(t)]^2dt, \tag{24}$$

where t_0 is the time required for acceleration of the rotor from zero to the desired speed ω, and $\omega(t)$ is the variation of ω with time during the acceleration period. If one assume a constant rate of acceleration, the correction Δt is one-third of t_0 [cf. Schachman, 1959]. Adding Δt to the time after the desired speed is attained would give the effective time of centrifugation.

The values of $M_{app}(t)$ from the meniscus and the bottom usually differ from each other and both of them vary with time, except when the solution is a monodisperse and ideal. According to the theory, both of them should merge to the same value, M_{app}, (if the pressure effect is neglible) as the values are extrapolated to zero time.

There are at least two major effects responsible for the time dependence of $M_{app}(t)$ (Fujita et al., 1962; Inagaki et al., 1963; Toyoshima et al., 1964). One is the fractionation effect: when the solute is polydisperse, sedimentation concentrates heavier components at the bottom and thus tends to decrease $M_{app}(t)$ with time at the meniscus, and to increase its value at the bottom, as well. The other is the nonideality effect, which is explained as follows: When we just consider a monodisperse but nonideal solution, equation (11) then reduces to

$$M_{app}(t)=M_1-M_1^2B_{11}c+0(c^2). \tag{25}$$

The value of c is denoted at the meniscus by c_m and at the bottom by c_b. If we write $c_m=c^0-\Delta c_m$, and $c_b=c^0+\Delta c_b$, both Δc_m and Δc_b are positively increasing functions of time. Substitution of the above equations into equation (25) gives

$$M_{app}(t)=M_{app}+M_1^2B_{11}\Delta c_m+0(\Delta c_m^2), \tag{26a}$$

$$M_{app}(t)=M_{app}-M_1^2B_{11}\Delta c_b+0(\Delta c_b^2), \tag{26b}$$

where M_{app} is the apparent molecular weight

$$M_{app}=M_1-M_1^2B_{11}c^0+0(c^{02}). \qquad (26c)$$

From these equations it follows that the value of $M_{app}(t)$ increases with time at the meniscus and decreases at the bottom, provided the nonideality parameter B_{11} is positive, i.e., when a good solvent is employed. Thus we see that the nonideality effect can give rise to a time dependence of $M_{app}(t)$ just opposite to that of the fractionation effect.

Yphantis (1959) examined the fractionation effect by calculating $M_{app}(t)$ for an ideal system consisting of equal amount of two solutes with different molecular weights with use of Mason and Weaver (1924) equation. He pointed out that the plot of the values of $M_{app}(t)$ against the square root of time is almost linear over a considerable range and provides satisfactory extrapolation to M_w.

On the nonideality effect, few quantitative examinations have been carried out. Some data to check this point was given by Inagaki and Kawai (1962), in which Δc_m was plotted as a function of the square root of time and also as a linear function of time for a polystyrene-methyl ethyl ketone system at 25°C. As seen in Fig. 7, the plot of Δc_m versus $\sqrt{t}$ gives a straight line over a considerable range. The result suggests that plotting $M_{app}(t)$ against $\sqrt{t}$ is better procedure than plotting it against t.

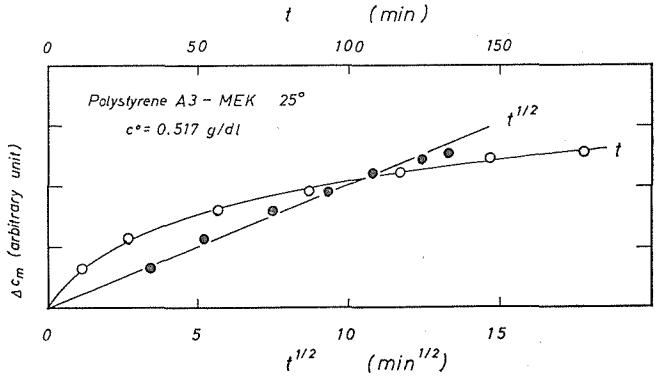

Fig. 7. An example of plot of Δc_m versus $\sqrt{t}$ and t (cf. equation 26a). A polystyrene ($M_w=1.17\times10^5$)-methyl ethyl ketone (0.517 g/dl) system was centrifuged at 25° with 10,672 rpm. (Inagaki and Kawai, 1962).

With polydisperse, nonideal systems various types of time dependence of $M_{app}(t)$ can be expected depending on the relative importance of these two effects. The most reliable procedure for extrapolation is still to be worked out. In most of the data presented so far, either the extrapolation of $M_{app}(t)$ with respect to time was just disregarded, or the values of $M_{app}(t)$ were plotted simply against time and the apparent molecular weight, M_{app}, was obtained by free hand extrapolation. Fig. 8 shows the plots of $M_{app}(t)$ versus t from both ends obtained with a mixture of ribonuclease and sucrose (Ginsburg et al., 1956). Here $M_{app}(t)$ is seen to be decreasing with time at the meniscus and increasing at the bottom. Fig. 9 shows the similar plots

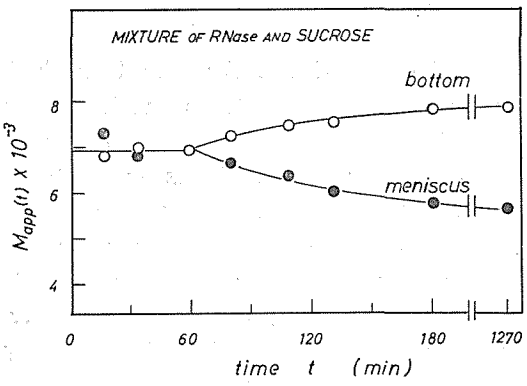

Fig. 8. Time dependece of $M_{app}(t)$ for the meniscus (●) and the bottom (○). A mixture of ribonuclease (M=14,000) and sucrose (M=342.3) in aqueous solution was centrifuged with 11,150 rpm. Theoretical molecular weight of this mixture was 6,960. For these calculations it was assumed that the refractive-increments for both components are the same and an average value of $(1-\bar{v}\rho)$ could be used (Ginsburg et al., 1956).

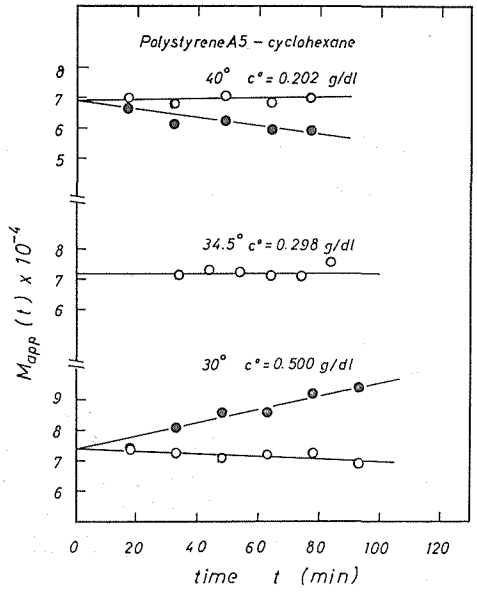

Fig. 9. Time dependence of $M_{app}(t)$ for the meniscus (○) and the bottom (●). A polystyrene (M_w=6.90×10^5)-cyclohexane system was centrifuged at three different temperatures near the θ-temperature, 34.5°: (a) initial concentration c^0=0.202 g/dl, rotor speed=18,137 rpm., temperature T=40°; (b) c^0=0.298 g/dl, 16,299 rpm., T=34.4°; (c) c^0=0.500 g/dl, 15,620 rpm., T=30.0° (Inagaki et al., 1963).

obtained with a polystyrene (M_w=6.90×10^5)-cyclohexane system around the θ-temperature, 34.5°C (Inagaki et al., 1963). Above the θ-temperature where B is positive, $M_{app}(t)$ increases with time at the meniscus and decreases at the bottom. Below θ where B is negative, the tendency seems to be reversed (see also Toyoshima and Fujita, 1964).

IV. THE TRAUTMAN METHOD

An interesting modification of the Archibald method was proposed by Trautman (1956) for evaluating M_{app}. This method, named the Trautman method, consists of plotting a function of $(\partial\tilde{n}/\partial r)$ versus a fuction of concentration as obtained at either the meniscus or the bottom of the solution column. An advantage of this method is that an independent evaluation of $\tilde{n}^0$ is not required, although a composite of several runs at various speeds for a single solution is required to cover a wide region of variables. Further and more important advantages are, as pointed out by Trautman (1956) himself, that (i) more procision can be obtained and (ii) any deviation from a straight line in the Trautman plot would indicate polydispersity or the nonideality of the system to be studied.

The essential part of the Trautman method is to introduce such variables as

$$X=(\tilde{n})_{r1}-\tilde{n}^0=-(1/r_1^2)\int_{r_1}^{r_p} r^2(\partial\tilde{n}/\partial r)\,dr \tag{27a}$$

$$Y=(RT/\omega^2 r_1)(\partial\tilde{n}/\partial r)_{r1} \tag{27b}$$

(for the bottom data replace r_1 by r_2) and to plot X versus Y. One would readily see from equation (10) or (11) that any arbitrary unit can express the concentration.

By substituting these variables into equation (10) one obtaines

$$Y=M^*_{app}(t)[X+\tilde{n}^0] \tag{28}$$

where $M^*_{app}(t)$ is the equivalent to the right-hand side of equation (10).

By plotting X versus Y, various data for the solution at different speeds and time of centrifugation should fall on a single curve. We define the intercepts of this curve to the X and Y axes as the points X^0 and Y^0, respectively. It is clear that $X^0=-\tilde{n}^0$ and the slope of the line passing through X^0 and Y^0 corresponds to $M^*_{app}(0)$ as a function of n^0[$M^*_{app}=(1-\bar{v}\rho)M_{app}$ if $\bar{v}_i=\bar{v}$ for all i]. The slope of any line passing through X^0 and any point on the curve corresponds to $M^*_{app}(t)$ as shown schematically in Fig. 8. The shape of the curve should reflect both of the polydisperoity and nonideality of the solution. One can deduce the shape of this plot qualitatively for two extreme cases, i.e., (i) for a monodisperse, nonideal solution and (ii) for a polydisperse, ideal solution [Kotaka and Inagaki, (1961)].

For a monodisperse, nonideal solution equation (8) reduces to:

$$Y=\frac{M_1(1-\bar{v}_1\rho)}{1+c_1\dfrac{\partial \ln y_1}{\partial c_1}}(X+\tilde{n}^0) \tag{29}$$

Apparently at the θ-temperature where the nonideality vanishes, the X versus Y plot should give a straight line with the slope proportional to $(1-\bar{v}_1\rho)M_1$. Depending on whether the temperature is below or above θ ($\partial \ln y_1/\partial c_1$ is negative or positive) the curve should be concave upward or downward, respectively, as schematically shown in Fig. 10a. The slope of the tangent to

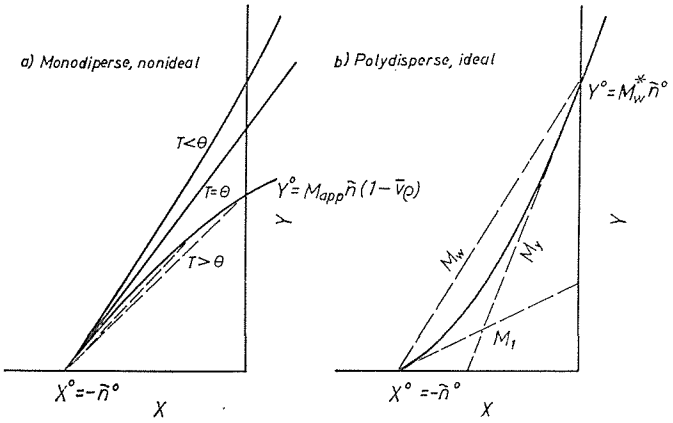

Fig. 10. Schematic diagram for the Trautman plot. (a) A monodisperse, nonideal solution : molecular weight of the solute is M. (b) A polydisperse, ideal solution : molecular weight of the smallest solute is M_1. The average molecular weight defined by equation (32) is referred to as M_Y.

the curve at X^0 should be proportional to $(1-\bar{v}_1\rho)M_1$.

For a polydisperse, ideal solutions equation (10) reduces to

$$Y=(\sum_{i=1}^{q} R_i M^*_i c_i/\sum_{j=1}^{q} R_i c_i)(X+\hat{n}^0). \tag{30}$$

The fractionation effect should tend to decrease the $M^*_{app}(t)$ with time at the meniscus and increase it at the bottom because of the accumulation of heavier components at the bottom. The curve should always be concave upward as shown shematically in Fig. 10b. For the evaluation of the polydispersity of the solute (dY/dX) would be an interesting parameter. Particularly, the value of (dY/dX) at the point Y^0 is of interest because it should reflect the polydispersity of the initial solution.

Now assuming the curve is plotted from a series of data at different times, taking time t as an auxiliary variable one can obtain the relation (see Yphantis, 1959)

$$(dY/dX)=\sum_{i=1}^{q} R_i M^*_i(\partial c_i/\partial t)/\sum_{i=1}^{q} R_i(\partial c_i/\partial t). \tag{51}$$

To derive a quantitative relation one has to know the form of $c_i(t)$ as a function of t. Unfortunately no exact solution has been given so far, but some approximate solutions are avairable (Mason and Weaver, 1924; Archibald, 1938 1942; Nazarian, 1958; Fujita and MacCosham, 1959). Using of any one of such solutions and taking the limit of $t=0$, one obtains the equation (see Yphantis, 1959; Erlander et al., 1960)

$$(dY/dX)_{Y^0}=\sum_{i=1}^{q} R_i M^*_i(s_i/D_i^{1/2})c_i^0/\sum_{i=1}^{q} R_i(s_i/D_i^{1/2})c_i^0. \tag{32}$$

Here s_i and D_i, the sedimentation and diffusion coefficients of solute i, are assumed to be independent of concentration; thus there is no interaction between solute molecules.

The type of average molecular weight one can expect to obtain from $(dY/dX)_{Y^0}$ depends on what type of molecular weight dependence the factor $(s/D^{1/2})$ of the solute in question shows. For example, for a rigid sphere model s is proportional to $M^{2/3}$ and $1/D$ to $M^{1/3}$, therefore, $(s/D^{1/2})$ to $M^{5/6}$; for a flexible linear chain at the θ temperature s is proportional to $M^{1/2}$ and so is $1/D$, therefore $(s/D^{1/2})$ to $M^{3/4}$; for a rodlike model s is proportional to $M^{1/5}$ and $1/D$ to $M^{4/5}$, therefore, $(s/D^{1/2})$ to $M^{3/5}$. One can deduce these figures from the calculations of the translational friction coefficient for each model (see, for example, Tanford, 1961). In any event one might say that (s/D) is proportional to M and if s is regarded as proportional to M^a, the power a may vary at most from 0 to 1. Therefore $(s/D^{1/2})$ should be proportional to a power of M between 1 and 1/2. An average molecular weight thus obtained would be one between M_z and 1.5th power average of M as far as the assumption cited above remains valid for the system in question.

The value of (dY/dX) at the point X^0 would reflect the value of the smallest solute-component. This point was established by Erlander et al. (1959) and also discussed theoretically by Yphantis (1959).

The nonideality and the fractionation effects on the Trautman plot were clearly demonstrated in our preliminary experiment with the polystyrene-cyclohexane system [Kotaka and Inagaki (1961)]. Results are shown in Fig. 11a and 11b. In these figures $Y/(1-\bar{v}\rho)$ was plotted against X, because this plot is more convenient in that the slope would be directly proportional to molecular weight. (It is assumed that $R_i=\overline{R}$, $\bar{v}_i=\bar{v}$ for all solutes).

For the test of the nonideality effect a polystyrene sample of $M_w=4.76\times$

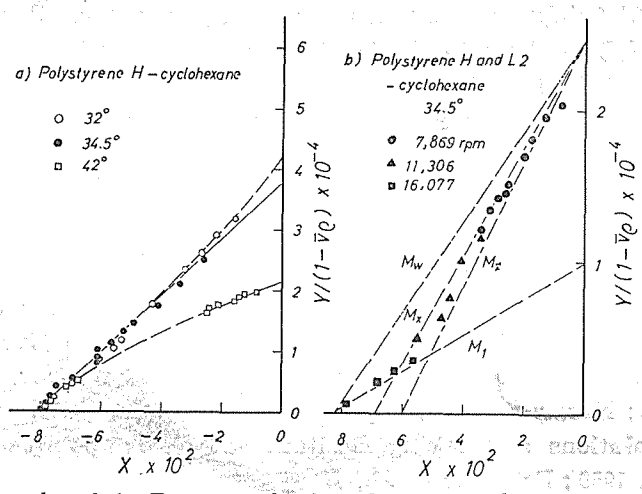

Fig. 11. Examples of the Trautman plot for polystyrene-cyclohexame system. (a) Polystrene $H(M_w=4.76\times10^5)$ at temperatures as indicated. The initial concentration is 0.483 g/dl. (b) A one to one (by weight) mixture of polystyrene L2 ($M_w=1.20\times10^5$) and H measured at 34.5°. The initial concentration is 0.496 g/dl. Calculated average molecular weights are: $M_w=2.98\times10^5$; the 1.5th power average of M (referred to as M_X) $=3.57\times10^5$; $M_Z=4.04\times10^5$. Broken lines indicate the corresponding calculated ones. (Kotaka and Inagaki, 1961).

10^5, obtained by the usual technique of fractionating precipitation, was used. We could obtain reasonably good straight line at the θ-temperature, 34.5°C, as seen in Fig. 11a. The curve is concave upward below θ and concave downward above θ, as anticipated from the theory. The sample is only reasonably monodisperse, but nonideality is still an overwhelming factor and one sees little fracionation effect.

For the test of the fractionation effect, a one to one (by weight) mixture of two fractionated polystyrene samples (M_w: 4.76×10^5 and 1.20×10^5) was used. We obtained, as seen in Fig. 11b, an upward concavity. Calculated lines corresponding to M_w, M_z, 1.5th power aveage of M and M_1 (of the smaller component) are also shown in the figure. The slope near X^0 seems to be fairly close to 1.20×10^5. It is hard to say what type of an average molecular weight was actually obtained here, because the differences between them are not large in this system. It looks, however, unlikely that the obtained average is M_z.

V. EXAMPLES OF APPLICATION OF THE ARCHIBALD METHOD

1. Study of Macromolecules from Natural Sources

The Archibald method has been applied to macromolecules of biological interest, particularly to proteins, with spectacular success. The reason for this success seems to be due in part to the fact that good preparations of proteins are usually quite monodisperse and in part that the nonideality can be reduced by a proper choice of the buffer system. In the case of the handling a monodisperse, ideal solution, a single sedimentation run under properly prescribed condition is sufficient to determine the molecular weight. Extrapolation of $M_{app}(t)$ with time is not necessary and there is also no need of studying concentration dependence of M_{app}, except when chemical reaction takes place in the system (Rao and Kegels, 1958).

Table 1 lists some results of the molecular weights of macromolecules from natural sources measured by the Archibald method. The values are also compared with the results obtained by some other methods. In all cases the coincidence seems to be quite good.

One of the interesting applications of this method is that for the study of chemically reacting systems (cf. Fujita, 1962, chapter IV). It has been known that association-dissociation takes place in many protein systems such as insulin, casin, α-chymotrypsin and some other enzymes.

In studying such systems by the Archibald method it should be noted that the flow equation (7) still remains valid. Naturally the boundary condition of the ultracentrifuge is also valid. Of course the continuity equation of the type of equation (4) is no longer valid for chemically reacting system, it needs an additional term to represent the rate of production of the component resulting from the reaction. For the Archibald method however this is not pertinent, but rather the only required conditions are the flow equation and the boundary condition. Therefore the discussion given in the

section III may be directly extended to any reacting system. The equation (11a) provides the $M_{app}(t)$ and after extrapolation to zero time M_{app} can be defined as a function of the initial concentration, provided all the solute compoents have the same partial specific volume and the same specific refractive index increment. In such a case equations (18a, b) for determining the values of $(\bar{n})$ at $r=r_1$ and r_2 are also valid (Kegels and Rao, 1958).

For a system with reversible polymerization and depolymerization reactions taking place, M_{app} gives the weight-average molecular weight, M_w, of the solutes corresponding to the solute composition at the particular initial concentration, c^0, provided the system is thermodynamically ideal. The weight-average values of M_w are a function of the initial concentration. By determining the relation of M_w versus c^0 one can evaluate the molecular weight of the monomer from the value of M_w at $c^0=0$, as well as the polymerization constants. A demonstration of this was given by Rao and Kegels (1958) with α-chymotrypsin in phosphate buffer (pH=6.2 and ionic strength I=0.2) system.

2. Study of Synthetic Macromolecules

Data of interset here are the values of M_{app} as a function of the initial concentration, c^0. The plot of $1/M_{app}$ versus c^0 gives the weight-average molecular weight, M_w, from the intercept at $c^0=0$ and the light scattering second virial coefficient from the initial slope (cf. equation 12). Fig. 12 shows the results obtained by Inagaki et al. (1963) for a polymethyl methacrylate-n-butyl chloride system around the θ-temperature. Here one sees as the temperature goes down the value of B varies from positive to zero (at the θ-temperature), to negative. Fig. 13 shows the results obtained by Inagaki and Kawai (1964a) for a polystyrene-benzene system at 25°C, in which direct comparison was made to the data obtained by the light scattering method. The coincidence between the two seems to be fairly good at the low concentration region, but a slight discrepancy is seen in the high concentration region. Also some more results obtained by Inagaki and Kawai (1964a) are shown in Fig. 14 for polystyrene-methyl ethyl ketone systems at 25°C.

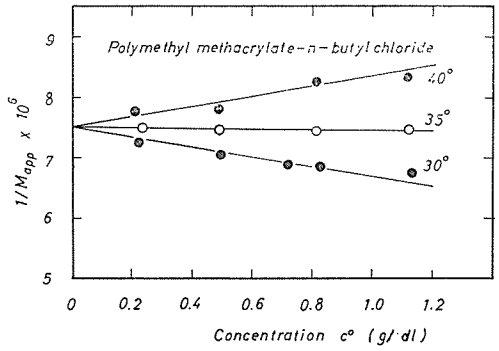

Fig. 12. The plots of $1/M_{app}$ versus c^0 for a polymethyl methacrylate ($M_w=1.32\times10^5$)-n-butyl chloride system around the θ-temperature, 35.5°. (Inagaki et al., 1963).

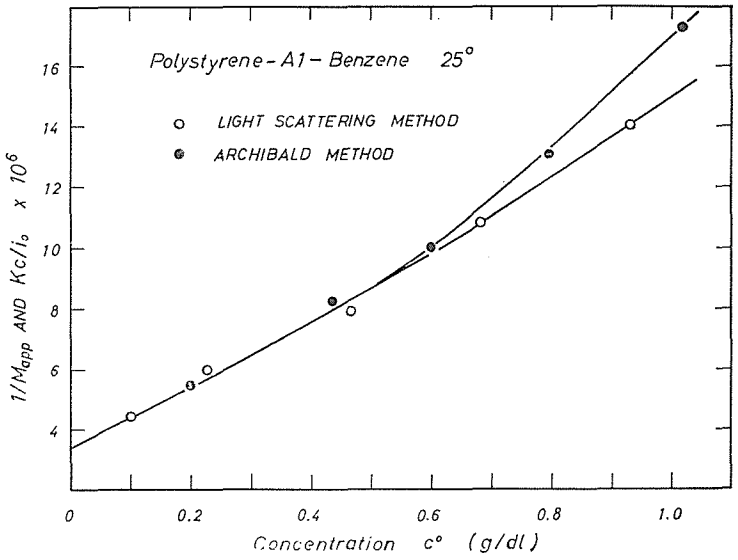

Fig. 13. Comparison of the Archibald data (●), $1/M_{app}$ versus c^0, and the light scattering data (○), Kc^0/i_0 versus c^0, for a polystyrene A1 ($M_w=3.09\times10^5$)-benzene system at 25° (Inagaki and Kawai, 1964a).

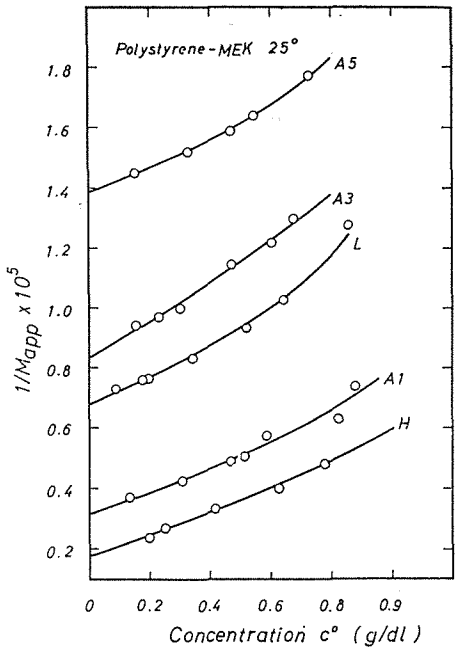

Fig. 14. The plots of $1/M_{app}$ versus c^0 for polystyrene-methyl ethyl ketone systems at 25°. (Inagaki and Kawai, 1964a).

In all cases in good solvent systems one sees rather high upward concavity in the plots. Also discrepancy is seen between the Archibald, and the light scattering, data (cf. Fig. 13) particularly at high conccentrations. The reason for this high curvature and the discrepancy has not been es-

tablished as yet. The present theory does not provide any reason why this should be so. The high curvature might be a true phenomenon or else might be due to artifacts in the ultracentrifugal experiments. Recently Toyoshima and Fujita (1964) suggested that high curvature could be due to the polydispersity of the solute.

In any case the high curvature in the plots of $1/M_{app}$ versus c^0 makes it difficult to obtain high precision in the extrapolation to zero concentration; this reduces the practical value of the plots of $1/M_{app}$ versus c^0. A semi-empirical procedure was proposed by Inagaki (1963) to avoid this difficulty; it consists of plotting $\ln(1/M_{app})$ versus c^0, instead of $1/M_{app}$, versus c^0

$$\ln(1/M_{app}) = \ln(1/M_w) + M_w B c^0 + \text{higher terms in } c^0. \qquad (33)$$

The pocedure would give a straight line in the case where the coefficient of the $(c^0)^2$ term in equation (12) is approximately equal to $2M_w(A_2')^2$. The data in Fig. 14 are replotted in Fig. 15 by employing this procedure. This yields fairly good straight lines over a considerable range, and it enables one to evaluate easily the values of the intercept and initial slope. Table 2 lists some of the results obtained for synthetic macromolecules with both the Archibald and light scattering methods. The coincidence seems to be fairly good between the values obtained by both methods.

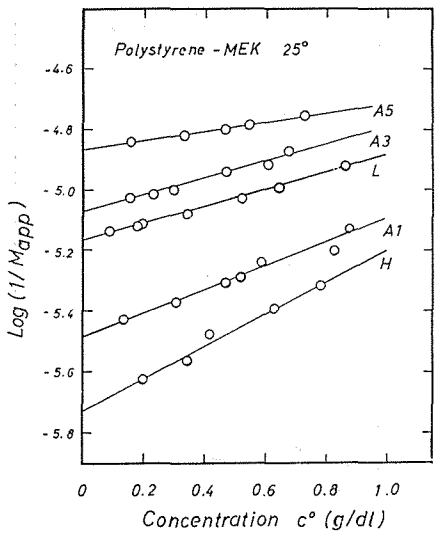

Fig. 15. Plots of $\log(1/M_{app})$ versus c^0 for polystyrene-methyl ketone systems at 25°. Replotted from the data shown in Fig. 14. (Inagaki and Kawai, 1964a).

Table 3 lists the systems of synthetic macromolecles which have been studied so far.

With the Archibald method one requires only a small amount of the material, and measurements can be made rapidly with fair accuracy. This is particularly advantageous in handling a, in some way, unstable system such that the solute and or the solvent dislike to be brought into contact

with oxygen or with moisture in the air. It seems to be rather easy to introduc the solution into a centrifuge cell and to carry out an experiment keeping the sample from contact with the air. A further advantage is that one needs to take no great pains to clean the solution to be tested, while a clean solution is an essential requirement in the light scattering method.

The chief disadvantage of the Archibald method is lack of high precision because one needs to rely on data obtained by extrapolation to the ends of the solution column. Appearance of a steep concentration gradient at the ends inevitably introduces a certain ambiguity in the results. This is particularly true for a material with a large sedimentation coefficient, or in other words, a high molecular weight. And also for ultracentrifuges now available, there is a limit for the lowest speed at which the stable operation is possible (perhaps 5,000 rpm is the lower limit at the present moment). These facts set the higher limit to the molecular weight of solutes for which the Archibald method is practically applicable to somewhere of the order of 10^6. One should remember however that any other conventional methods of molecular weight determination are also not very reliable in this range.

Because of the advantages mentioned above, the Archibald method seems to be useful as a routine procedure for determining molecular weights and the light scattering second virial coefficients of macromolecules. Also the Archibald method could, perhaps, replace the light scattering method, except where one wishes to measure the conformation (radius of gyration) of macromolecules in solution.

Table 1. List of the results obtained by the Archibald method for proteins and other molecules from natural sources.

Material[a]	T°C	Buffer[c]	$\bar{v}$	M_w (Archibald)[e]	M_w (From s & D)[a]	Reference
ACTH peptide fractions						
A	25	0.3M NaCl	0.70	520	570	Li, et al. (1951)
B				410	410	
C				1000	1400	
Alcohol dehydrogenase (liver)	20	0.05M phosphate 1% NaCl; pH=7.0	0.750	84400	84000	Ehrenberg (1957)
Amylose FIA	25	0.5M KCl	0.65	2080000	2440000 (L)	Everett & Foster (1959)
Apomyoglobin	20	0.05M phosphate 1% NaCl ; pH=7.0	0.743	18800	18200 (F)	Ehrenberg (1957)
Apurinic acid	25	Na-acetate pH=5.0 ; I=0.15	0.55	27000	25000	Smith et al. (1950)
BSA	25	Na-acetate	0.7343	70300	67000–71000	Klainer & Kegels (1956)
	20	0.05M phosphate 1% NaCl pH=7.0	0.7343	73200	73500	Ehrenberg (1957)
	25	Na-acetate pH=4.4 ; I=0.2	0.7343	71000		Richards & Schachman (1959)
	25	0.1M NaCl	0.736	77500		Inagaki et al (1964c)
α-chymotrpsin		Na-phosphate pH=6.2 ; I=0.2	0.736	23000		Rao & Kegels (1958)

CO-myoglobin	20	0.05M phosphate 1% MaCl ; pH=7.0	0.743	18300	18200	Ehrenberg (1957)
L-cystine peptide	25	Ma-acetate; pH=4.5	0.61	231	222(F)	Wade et al. (1956)
Cytochrome C (beef heart)	20	0.05M phosphate 1% NaCl ; pH=7.0	0.728	13300	13300 (F)	Ehrenburg (1957)
Digtonin	4	63% EtOH	0.699	1310	1229(F)	Brown et al. (1954)
Glycyl-L-leucine	25	Na-acetate pH=4.5	0.74	185 ; 193	188(F)	Wade et al. (1956)
Heparin I	25	1M KCl	0.479	15800	15500	Patat & Elias (1959)
IV				13800	13700	
Histone (calfthymus) A		Na-acetate pH=5.5 ; I=0.1	0.765	*9850	20600 (F)	Trautman & Crampton (1959)
		+6M urea	0.765	*12800		
B		Na-acetate pH=5.5 ; I=0.1	0.746	*31500	19700 (F)	
		+6M urea	0.746	*16500		
α-ketosuccinamic acid		0.1N HCl		260	262(F)	Otani et al. (1954)
				130	131(F)	
β-loctoglobulin	23.5	Na-acetate pH=5.2 I=0.2	0.75	35400	35400	Ginsburg et al. (1956)
Lysozyme	25	Na-phosphate pH=6.6 ; I=0.2	0.688	14100	14100	Smith et al. (1956)
poly-DL-lysyl-l-tyrosine	25	0.2M NaCl	0.879	23700	23900	Micheel et al. (1960)
Myloperoxidase	20	0.05M phosphate 1% NaCl pH=7.0	0.731	157000	145000	Ehrenberg (1957)
OYE	20	0.05 phosphate 1% NaCl pH=7.0	0.753	106000	106000	Ehrenberg (1957)
Raffinose	25	Na-acetate pH=4.4 ; I=0.2	0.6077	505	504.4 (F)	Kleiner & Kegels (1955)
Rhodanese	20	0.05M phosphate 1% NaCl ; pH=7.0	0.741	35300	35600	Ehrenberg (1957)
s-RNA from brewery's yeast	25	0.1M Tris, 0.1M KCl ; pH=7.4	0.51	23000		Utiyama et al. (1963)
RNase	25		0.709	14000	13895 (F)	Ginsburg et al. (1956)
	25	0.1M NaCl 0.004M KH_2PO_4 0.035M K_2HPO_4 pH=7.8	0.709	14000	13000 13400 (X)	Klainer & Kegels (1956)
	24	0.1M NaCl pH=5.7 −6.6 I=0.1	0.695	13500		Erlander & Foster (1959)
		Na-acetate pH=5.5 ; I=0.1	0.692	*14000		Trautman & Crampton (1959)
		+6M urea		*12500		
Sucrose	25	water		348.3	342.3 (F)	LaBar (1963)

a) In this column : ACTH=adrenocorticotropic hormone ; BSA=bovine serum albumin ; OYE=old yellow enzyme ; s-RNA=soluble ribonucleic acid ; RNase=ribonuclease.

d) In this column : I=ionic strength.

e) In this column : (*) indicates the Trautman procedure was employed.

d) In this column : the values are those by separate measurements of s and D unless otherwise specified. (F)=fomula value or those by chemical analysis ; (L)=light scattering ; (X)=X-ray analysis.

Table 2. Comparison of the results obtained by the Archibald and the light scattering method for synthetic macromolecules.

Polymer	T°C	Solvent[a]	$M_w \times 10^{4}$[b] (A)	$M_w \times 10^{4}$[b] (LS)	$A'_2 \times 10^{-4}$[b] (A) (c. g. s.)	$A'_2 \times 10^{-4}$[b] (LS) (c. g. s.)	Reference
Rolyethylene	115	α-Cl-naphthalene	12.6	14.4	11.5	8.6	Weston & Billmayer (1963)
Polyethyleneglycol H 10000	25	water	1.09	1.20	116[c]	114[c]	Elias (1961a)
Polystyrene							
H-PSt	25	MEK	47.6	49.6	1.35	1.75	Fujita et al. (1962)
L-PRt	25	MEK	14.3	12.7	1.34	1.92	
PSt-A1	25	Benzene	26.3	25.6	3.0	3.6	Inagaki & Kawai (1964a)
SM 1	25	MEK	28.2	27.9	1.37	1.54	Toyoshima & Fujita (1964)
SM 1	35	CH	28.2	28.9	0	0	
S 111	25	MEK	22.2	20.4	1.75	2.1	
S 111	35	CH	22.2	26.5	0	0	

[a] MEK=methyl ethyl ketone : CH=cyclohexane.
[b] (A)=the Archibald method : (LS)=the light scattering method.
[c] The sedimentation equilibrium method was used instead of the light scattering method. The unit is (atm $cm^6 g^{-2}$).

Table 3. List of synthetic macromolecules studied by the Archibald method.

Macromolecules	solvent[a]	T°C	$\bar{v}$	Reference
Polyacrylonitrile	DMF	20	0.830	Scholtan & Marzolph (1962)
		25	0.830	Inagaki et al. (1961b)
Polyethylene	α-Cl-napthalene	115	1.254	Weston & Billmeyer (1963)
	n-Decane	115	1.211	
Polyethyleneglycol	water	25	0.820	Elias (1961)
				Ritscher & Elias (1962)
				Inagaki & Tanaka (1964d)
Polymethylmethacrylate	n-butylchloride	30	0.806	Inagaki et al. (1963)
		35	0.810	
		40	0.815	
	MEK	25	0.7993	
Polystyrene	benzene	25	0.917	Elias (1962)
				Inagaki & Kawai (1964a)
	cyclohexane	30	0.935	Inagaki et al. (1963)

		34.5	0.939	
		40.0	0.946	
		35	0.940	Toyoshima & Fujita (1964)
	MEK	25	0.907	Fujita et al. (1962)
				Inagaki & Kawai (1964)
				Toyoshima & Fujita (1964)
Polyvinylchloride	THF	25	0.7429	Kegels et al. (1967)

a) DMF=dimethyl formamide; MEK=methyl ethyl ketone; THF=tetrahydrofuran.

REFERENCES

(1) Archibald, W. J. (1938). *Phys. Rev.* **53**, 746 ; *Phys. Rev.*, 54, 371.
(2) Archibald. W. J. (1942). Ann. N. Y. Acad. Sci. **43**, 211.
(3) Archibald, W. J. (1947a). *J. Appl. Phys.* **18**, 362.
(4) Archibald, W. J. (1947b). *J. Phys. Colloid Chem.* **51**, 1204.
(5) Baldwin, R. L. (1959). unpublished expeeiments ; cited in Baldwin and Van (1960).
(6) Baldwin, R. L. and Van Hold, K. E. (1960). *Fortschr. Hochpolym. Forsch.* **1**, 451.
(7) Brown, R. A., Kritschevsky, D. and Davies, M. J. (1954) *J. Am. Chem. Soc.* **76**, 3342.
(8) Ehrenberg, A. (1957). *Acta Chem. scand.* **11**, 1257.
(9) Elias, H.-G. (1961a). *Angew. Chem.* **73**, 209.
(10) Elias, H.-G. (1961b). *Makromol. Chem.* **50**, 1.
(11) Elias, H.-G. (1962) *Makromole. Chem.* **54**, 78.
(12) Elias, H.-G. and Patat, F. (1960a). *Naturwiss.* **47**, 108.
(13) Elias, H.-G. and Patat, F. (1960b). *Z. physiol. Chem.* **319**, 22.
(14) Erlander, S. R. and French, D. (1950). *J. Polymer Sci.* **20**, 7.
(15) Erlander, S. R. and Foster, J. F. (1959). *J. Polymer Sci.* **37**, 103.
(17) Erlander, S. R., Koffler, H. and Foster, J. F. (1960). *Arch. Biochem. Biophys.* **90**, 139.
(18) Everett, W. B. and Foster, J. F. (1959). *J. Am. Chem. Soc.* **81**, 3458.
(19) Faxen, H. (1929). *Ark. Mat. Astron. Fysik.* **21B**, (3).
(20) Fick, A. (1855). *Ann. Physik u. Chem.* **94**, 59.
(21) Fujita, H. (1962). "Mathematical Theory of Sedimentation Analysis," Academic Press, New York.
(22) Fujita, H., Inagaki, H., Kotaka, T. and Utiyama, H. (1962). *J. Phys. Chem.* **66**, 4.
(23) Fujita, H. and MacCosham, V. J. (9159). *J. Chem. Phys.* **30**, 291.
(23) Ginsburg, A., Appel, P. and Schachman, H. K. (1956). *Arch. Biochem. Biophys.* **65**, 545.
(29) Hooyman, G. J. (1956a). *Physica* **22**, 751.
(30) Hooyman, G. J. (1956b). *Physica* **22**, 761.
(31) Hooyman, G. J., Holtan Jr., H., Mazur, P. and de Groot, S. R. (1953). *Physica* **19**, 1095.
(32) Inagaki, H. (1963). *Makromol. Chem.* **64**, 215.
(33) Inagaki, H. and Kawai, S. (1962). unpublished experiments.
(34) Inagaki, H. and Kawai, S. (1964a). *Makromol. Chem.* in press.
(35) Inagaki, H., Kawai, S. and Nakazawa, A. (1963). *J. Polymer Sci.* **A1**, 3303.
(36) Inagaki, H., Hayashi, K. and Matsuo, T. (1964b), *Makromol. Chem.* in press.
(37) Inagaki, H., Nakazawa, A. and Kotaka, T. (1964c). *J. Colloid Sci.* in press.
(38) Inagaki, H. and Tanaka, M. (1964d). *Makromol. Chem.* **74**, 145.
(39) Kegels, G. and Rao, M. S. N. (1958). *J. Am. Chem. Soc.* **80**, 5721.
(40) Kirkowood, J. G. and Goldberg, R. J. (1950). *J. Phys. Chem.* **18**, 54.
(41) Klainer, S. M. and Kegels, G. (1955). *J. Phys. Chem.* **59** 952.
(42) Klainer, S. M. and Kegels, G. (1956). *Arch. Biochem. Biophys.* **63**, 247.
(43) Kotaka, T. and Inagaki, H. (1961). unpublished experiments.
(44) LaBar, F. E. (1963). Ph. D. thesis, Stanford Univ.

(45) Li, E. H., Tiselius, A., K. O. Hagdahl, L. and Carstensen, H. (1951); *J. Biol. Chem.*, **190**, 317.
(46) Mason, M. and Weaver, W. (1924). *Phys. Rev.* **23**, 421.
(47) Micheel, F. and Hülsmann, H. L. (1960). *Chem. Ber.* **93**, 13.
(48) Mommaerts, W. F. M. and Aldrich, B. B. (1958). *Biochem. Biophys. Acta* 28, 627.
(49) Nazarian, G. M. (1958). *J. Phys. Chem.* **62**, 1607.
(50) Otani, T. T. and Meister, A. (1954). *J. Biol. Chem.*, **224**, 137.
(51) Patat, F. and Elias, H.-G. (1959). *Naturwiss.* **46**, 322.
(52) Peterson, J. M. and Mazo, R. M. (1961). *J. Phys. Chem.* **65**, 566.
(53) Rao, M. S. N. and Kegels, G. (1958). *J. Am. Chem. Soc.* **80**, 5724.
(54) Richards, E. G. and Schachman, H. K. (1956). *J. Phys. Chem.* **63**, 1578.
(55) Ritscher, T. A. and Elias, H.-G. (1959). *Makromol. Chem.* **30**, 48.
(56) Schachman, H. K. (1959). "Ultracentrifugation in Biochemistry", Academic Press, New York.
(57) Scholtan, W. and Marzolph, H. (1962). *Makromol. Chem.* **57**. 52.
(58) Smith, D. B., Wood, G. C. and Charlwood, P. A. (1956). *Canad. J. Chem.*, **34**, 364.
(59) Stockmayer, W. H. (1950). *J. Chem. Phys.* **18**, 58.
(60) Svedberg, T. (1925). *Kolloid-Z.* **36** 53.
(61) Svedberg, T. and Chirnoaga, E. (1926). *J. Am. Chem. Soc.* **50**, 1933.
(62) Svedberg, T. and Nichols, J. B. (1923a). *J. Am. Chem. Soc.* **45**, 2910.
(63) Svedberg, T. and Rinde, H. (1923b). *J. Am. Chem. Soc.*, **45**, 943.
(64) Svedberg, T. and Pedersen, K. O. (1940). "The Ultracentrifuge", Clarendon Press, Oxford.
(65) Tanford, C. (1961). "Physical Chemistry of Macromolecules," chapter 6, John Wiley and Sons, New York.
(66) Toyoshima, Y. and Fujita, H. (1964). *J. Phys. Chem.* to be published.
(67) Trautman, R. (1956). *J. Phys Chem.* **60**, 1211.
(68) Trautman, R. and Crampton, C. F. (1959). *J. Am. Chem. Soc.* **81**, 4036.
(69) Utiyama, H. Kawade, Y. and Ozaki, M. (1963). unpublished experiments.
(70) Van Holde, K. E. and Baldwin, R. L. (1958). *J. Phys. Chem.* **62**, 734.
(71) Vinograd, J. and Hearst, J. E. (1962). *Forstschr. Chem. org. Naturstoffe* **20**, 373.
(72) Wade, R., Winittz, H. and Greenstein, J. P., (1956). *J. Am. Chem. Soc.* **78**, 373.
(73) Weston, N. E. and Billmeyer, F. B. (1963). *J. Phys. Chem.* **67**, 2728.
(74) Williams, J. W., Holde, K. E., Baldwin, R. L. and Fujita, H. (1958) ; Chem. Rev., 58, 715.
(75) Yphatis, D. A. (1959). *J. Phys. Chem.* **63**, 1742.